Atmos. Chem. Phys., 16, 11465–11475, 2016
www.atmos-chem-phys.net/16/11465/2016/
doi:10.5194/acp-16-11465-2016

Atmospheric Chemistry and Physics Open Access EGU

Trends in atmospheric ammonia at urban, rural, and remote sites across North America

Xiaohong Yao[1] **and Leiming Zhang**[2]

[1]Lab of Marine Environmental Science and Ecology, Ministry of Education, Ocean University of China, Qingdao 266100, China
[2]Air Quality Research Division, Science and Technology Branch, Environment and Climate Change Canada, 4905 Dufferin Street, Toronto, Ontario, M3H 5T4, Canada

Correspondence to: Xiaohong Yao (xhyao@ouc.edu.cn) and Leiming Zhang (leiming.zhang@canada.ca)

Received: 26 March 2016 – Published in Atmos. Chem. Phys. Discuss.: 23 May 2016
Revised: 28 August 2016 – Accepted: 31 August 2016 – Published: 14 September 2016

Abstract. Interannual variabilities in atmospheric ammonia (NH_3) during the most recent 7–11 years were investigated at 14 sites across North America using the monitored data obtained from NAPS, CAPMoN and AMoN networks. The long-term average of atmospheric NH_3 ranged from 0.8 to 2.6 ppb, depending on location, at four urban and two rural/agricultural sites in Canada. The annual average at these sites did not show any deceasing trend with largely decreasing anthropogenic NH_3 emission. An increasing trend was actually identified from 2003 to 2014 at the downtown Toronto site using either the Mann–Kendall or the ensemble empirical mode decomposition method, but "no" or "stable" trends were identified at other sites. The ∼ 20 % increase during the 11-year period at the site was likely caused by changes in NH_4^+–NH_3 partitioning and/or air–surface exchange process as a result of the decreased sulfur emission and increased ambient temperature. The long-term average from 2008 to 2015 was 1.6–4.9 ppb and 0.3–0.5 ppb at four rural/agricultural and at four remote US sites, respectively. A stable trend in NH_3 mixing ratio was identified at one rural/agricultural site while increasing trends were identified at three rural/agricultural (0.6–2.6 ppb, 20–50 % increase from 2008 to 2015) and four remote sites (0.3–0.5 ppb, 100–200 % increase from 2008 to 2015). Increased ambient temperature was identified to be a cause for the increasing trends in NH_3 mixing ratio at four out of the seven US sites, but what caused the increasing trends at other US sites needs further investigation.

1 Introduction

Atmospheric ammonia (NH_3) plays an important role in formation of ammonium sulfate and nitrate aerosols in the size range of nanometer to supermicron (Yao et al., 2007; Kulmala et al., 2004; Ianniello et al., 2011; Yao and Zhang, 2012; Schiferl et al., 2014; Paulot and Jacob, 2014). The sum of sulfate, nitrate, and ammonium ions (NH_4^+) usually consists of the major portion of $PM_{2.5}$ across Canada and the United States (Dabek-Zlotorzynska et al., 2011; Hand et al., 2012). With significant decreases in acidic gas emissions in the last decades across North America (e.g., emissions of SO_2 and NO_x in Canada decreased from 2.28×10^6 and 2.72×10^6 t year^{-1} in 2003 to 1.23×10^6 and 2.06×10^6 t year^{-1} in 2013, respectively (http://www.ec.gc.ca/inrp-npri/donnees-data/ap/index.cfm?lang=En)), more attention is being paid to the relationship between NH_3 and NH_4^+ aerosols (Zhang et al., 2010; Day et al., 2012; Nowak et al., 2012; Yao and Zhang, 2012; Schiferl et al., 2014; Zhu et al., 2013; Markovic et al., 2014; Paulot and Jacob, 2014).

NH_3 mixing ratios are affected by several factors such as NH_3 emissions, NH_3–NH_4^+ partitioning, and meteorological conditions (Sutton et al., 2009; Yao and Zhang, 2013; Hu et al., 2014). In Europe, previous studies showed that the long-term trend in atmospheric NH_3 observed in some countries did not reflect the dramatic decrease in NH_3 emissions and the phenomenon was referred to as "ammonia gap" (Sutton et al., 2009; Ferm and Hellsten, 2012; Sintermann et al., 2012). Long-term trends in atmospheric NH_3 across North America are poorly understood (Zbieranowski and Aherne, 2011; Hu et al., 2014; Van Damme et al., 2014).

Such knowledge is important for accurate prediction of ammonium sulfate and nitrate aerosol levels in the future (Pye et al., 2009; Walker et al., 2012). In North America, established anthropogenic NH_3 emission inventories showed that agricultural emissions accounted for over 80 % of the total anthropogenic NH_3 emissions (Lillyman et al., 2009; Behera et al., 2013; Xing et al., 2013). However, agricultural emission sources only affect mixing ratios of atmospheric NH_3 at short downwind distances (Theobald et al., 2012; Yao and Zhang, 2013). Non-agricultural emissions such as those from local traffic, waste containers, and soil and vegetation were reported to be important contributors to NH_3 in urban atmospheres (Whitehead et al., 2007; Ellis et al., 2011; Reche et al., 2012; Sutton et al., 2013; Yao et al., 2013; Hu et al., 2014), although these sources only accounted for a few percentage of the total NH_3 emissions in Canada and the United States. Due to new technology adopted, traffic-derived NH_3 decreased gradually (Bishop et al., 2010; http://www.ec.gc.ca/inrp-npri/donnees-data/ap/index.cfm?lang=En). Yao et al. (2013) and Hu et al. (2014) recently reported that traffic-derived NH_3 was a negligible contributor to atmospheric NH_3 in Toronto. However, under climate warming, soil and vegetation NH_3 emissions are expected to increase accordingly. For example, NH_3 volatilization potential nearly doubles under every 5°C increase (Pinder et al., 2012; Sutton et al., 2013; Fowler et al., 2015).

Atmospheric NH_3 and ammonium sulfate and nitrate aerosols can be transported downwind and eventually deposited to natural ecosystems to enhance carbon fixation (Krupa, 2003; Beem et al., 2010; Walker et al., 2012). Excessive NH_3 deposition may cause adverse effects such as reduced biodiversity and eutrophication (Krupa, 2003; Erisman et al., 2007; Beem et al., 2010; Bobbink et al., 2010; Pinder et al., 2012). Recent evidence shows changes in species composition for sensitive vegetation types at the annual average concentration of $1\,\mu g\,m^{-3}$ NH_3 (Cape et al., 2009). Climate warming may increase the vulnerability of ecosystems towards exposure to NH_3 (Pinder et al., 2012). Thus, trend analysis of atmospheric NH_3 at remote sites will help to better understand its potential impacts on sensitive natural ecosystems.

In this paper, interannual variabilities in atmospheric NH_3 at 14 sites across Canada and the United States were investigated, with particular attention paid to its long-term trends and causes. The 14 sites include 4 urban sites, 4 remote sites and 6 rural/agricultural sites distributed at different latitudes. Two trend analysis tools, i.e., the Mann–Kendall (M–K) analysis (Gilbert, 1987) and the ensemble empirical mode decomposition (EEMD, Wu and Huang, 2009), were used to resolve the time series of atmospheric NH_3 in mixing ratio at these sites. The analysis results provided new light on the long-term trends in atmospheric NH_3 at various sites across North America.

2 Methodology

2.1 Data sources of atmospheric NH_3

In this study, mixing ratios of atmospheric NH_3 generated at monthly interval were compiled from three data sources, i.e., the Canadian National Air Pollution Surveillance (NAPS, http://www.ec.gc.ca/rnspa-naps/) network, the Canadian Air and Precipitation Monitoring Network (CAPMoN; http://www.ec.gc.ca/natchem/default.asp?lang=En&n=90EDB4BC-1), and the US Passive Ammonia Monitoring Network (AMoN, http://nadp.sws.uiuc.edu/AMoN). Missing data are a common problem during long-term observations. The sites chosen in this study were based on data availabilities as detailed below.

The NAPS network provides accurate and long-term air quality data across Canada. At each site, a Partisol Model 2300 sequential speciation sampler (Thermo Scientific) equipped with dry denuders is used to measure concentrations of NH_3 and acidic gases and particulate chemical components such as pNH_4^+ and pNO_3^- in $PM_{2.5}$. The sampler maintains a constant flow rate of $10\,L\,min^{-1}$ and operates for a 24 h duration on every third day. The 24 h integrated denuder and filter samples were carried back to the lab where they were extracted and analyzed by ion chromatography (Dabek-Zlotorzynska et al., 2011). At a few sites, technical problems resulted in NH_3 and pNH_4^+ concentration data missing for several months. At four urban sampling sites and one rural/agricultural site (Fig. 1), the measurements allowed obtaining continuous time series of monthly averaged concentrations of atmospheric NH_3 and pNH_4^+ and were thereby used for trend analysis. However, these sites also suffer from the problem of missing data. For example, there were only 70–90 % months when 8–10 sets of 24 h data were available to calculate the monthly average value (Fig. S1 in the Supplement). This may cause uncertainty on the calculated trends in atmospheric NH_3 and pNH_4^+. Moreover, one site at Egbert in the southern Ontario (Fig. 1), the part of CAPMoN, also had the long-term measurement concentrations of atmospheric NH_3 and pNH_4^+ using the identical sampler as used in the NAPS network. The site is located in a rural/agricultural area. The data were also averaged monthly for the trend analysis. The six Canadian sites were referred to as Sites 1–6 on the basis of their annual average mixing ratios of atmospheric NH_3 in decreasing order.

The AMoN within the National Atmospheric Deposition Program in the United States started operation in fall 2007. An important objective of AMoN is to assess long-term trends in NH_3 concentrations and its deposition. AMoN included only 16 sites in 2007, and dozens of sites are now available. The Radiello® passive samplers are deployed every 2 weeks at each site according to the standard operating procedure for monitoring atmospheric NH_3. Puchalski et al. (2015) recently compared the bi-weekly passive measurements with those measured by annular denuder systems

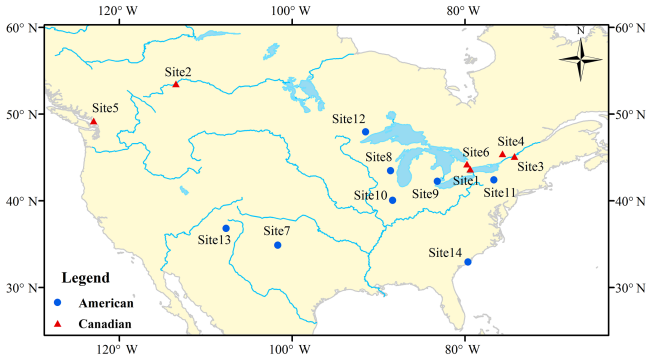

Figure 1. Map of 14 long-term atmospheric NH_3 monitoring sites across North America (NAPS Sites 1–5, CAPMoN Site 6 and AMoN Sites 7–14).

(ADSs) at several AMoN sites and found that the mean relative percentage difference between the ADS and AMoN sampler was −9 %. In this study, mixing ratios of atmospheric NH_3 at eight AMoN sites were selected for the trend analysis on the basis of two criteria (Fig. 1): (1) the length of the valid data should be at least 7 years according to Walker et al. (2000), and (2) there were no monthly average data missing each year. The eight sites were referred to as Sites 7–14 (Fig. 1), four of which were located in rural areas and another four in remote areas. Consistent with the six sites across Canada, the monthly averages at the eight sites were used for data analysis if not specified. Moreover, all ambient temperature (T) data were obtained from on-site records or nearby meteorological stations.

2.2 Statistical methods

The M–K analysis is a non-parametric statistical procedure which can be used to analyze trends in data sets including irregular sampling intervals, data below the detection limit, and trace or missing data (Kampata et al., 2008). Considering that the data flaws aforementioned were indeed present in our selected data sets to a certain extent, the M–K analysis is thereby used to resolve the time series of the annual average of NH_3 in this study. According to the analysis, the time series of n data points and T_i and T_j as two subsets of data where $i = 1, 2, 3, \ldots n-1$ and $j = i+1, i+2, i+3, \ldots n$ are considered. The series of data is used to calculate S'' statistic, confidence factor and coefficient of variation. The calculated values were further used to test the null hypothesis H_0 assuming that there is no trend and the alternative hypothesis H_1 assuming that there is a trend, yielding qualitative trend results such as "increasing/decreasing", "probable increasing/decreasing", "stable", and "no trend" (Gilbert, 1987). Moreover, the EEMD is a recently developed statistical tool to determine the trend of a time series of a variable in various fields such as economics, health, environment, and climate (Wu and Huang, 2009). The EEMD built on Empirical Mode Decomposition (EMD) and was updated by Wu and Huang (2009) to overcome the problem of mode mixing in the EMD. The method has since been applied widely (e.g., Erturk et al., 2013; Ren et al., 2014) because it is most suitable for resolving non-stationary and non-linear signals. The mixing ratio of atmospheric NH_3 was affected not only by its emissions, atmospheric transport, dilution, and deposition but also by non-stationary and non-linear chemical reactions (Ianniello et al., 2011; Hu et al., 2014). Thus, the EEMD is also used in this study and is briefly introduced here.

In general, all data are amalgamations of signal and noise as shown below:

$$X(t) = S(t) + N(t), \quad (1)$$

where $X(t)$ is the record data, and $S(t)$ and $N(t)$ are the true signal and noise, respectively. In the EMD, any data set is assumed to consist of different simple intrinsic modes of oscillations. Each of these intrinsic oscillatory modes is represented by an intrinsic mode function (IMF). In the EEMD, white noise is added to the single data set, $X(t)$, and the ensemble mean is used to improve accuracy of measurements.

3 Results and discussion

3.1 Temporal variations of atmospheric NH_3 at the six Canadian sites

Figure 2 shows monthly variations of atmospheric NH_3 in mixing ratio at the six Canadian sites. At Site 1, an urban site in downtown Toronto, the measured mixing ratios were 2.6 ± 1.2 ppb (average ± standard deviation) during the period from July 2003 to June 2014 (Fig. 2a and Table 1). When compared with those reported in other urban atmospheres, the long-term average value of 2.6 ppb ranked at a moderately low concentration level (Whitehead et al., 2007; Saylor et al., 2010; Alebic-Juretic, 2008; Meng et al., 2011). Interannual variations were evident at Site 1 with the coefficient of variation (CV) of 0.11, defined as the ratio of the standard deviation to the average. It should be noted that the annual averages in 2004 and 2005 were calculated from July 2003 to June 2004 and from July 2004 to June 2005, respectively, instead of a calendar year, in order to obtain the longest time series of annual averages. The similar calculations were used for other years and other sites. The M–K analysis result suggested an increasing trend from 2004 to 2014 with a confidence level of 98 %. When intra-annual variations were analyzed at Site 1, a distinctive seasonal trend was obtained with the highest seasonal average value of 3.7 ± 0.7 ppb in summer (June to August) and the lowest of 1.3 ± 0.6 in winter (December to the next February).

The M–K analysis results showed either "no" or "stable" trends in atmospheric NH_3 at the other Canadian sites with long-term average of 2.4 ± 0.6 ppb at Site 2, 2.1 ± 1.2 ppb at Site 3, 1.9 ± 0.8 ppb at Site 4, 1.6 ± 0.5 ppb at Site 5, and

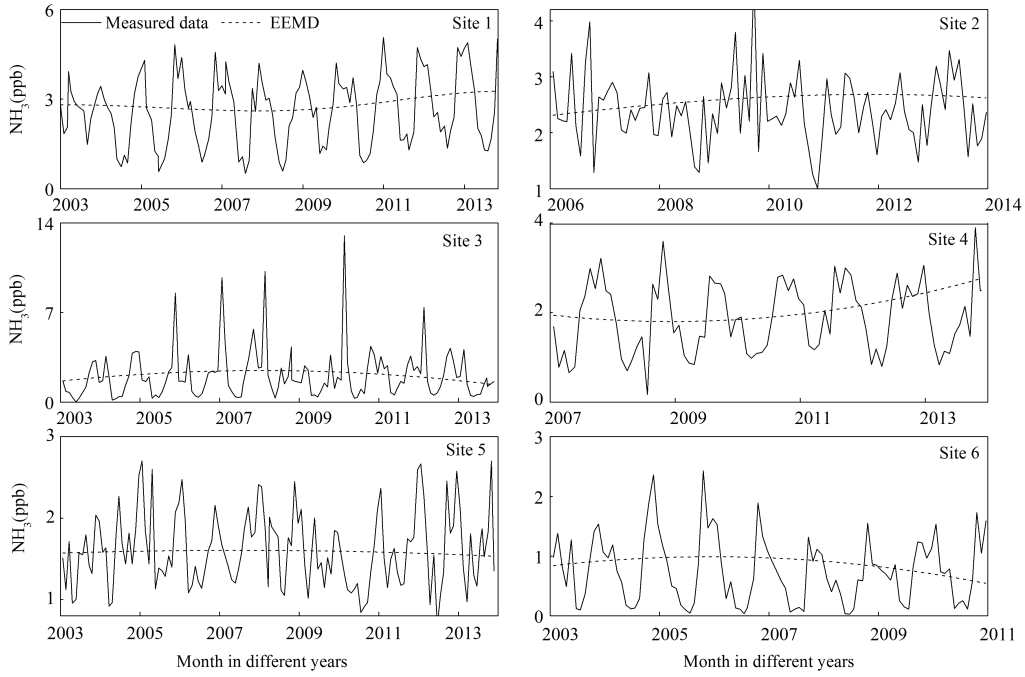

Figure 2. Monthly averages of measured atmospheric NH_3 and its long-term trends extracted using the EEMD at six Canadian sites.

0.8 ± 0.6 ppb at Site 6 (Fig. 2b–f). However, interannual variations at these sites were evident. For example, the CV values calculated from annul averages varied from 0.07 to 0.19, depending on location (Table 1). Atmospheric NH_3 at Sites 3, 4, and 6 exhibited a distinctive seasonal variation, but this was not the case at Sites 2 and 5. The largest seasonal variation occurred at Site 3 while the smallest occurred at Site 2. The two sites were selected as examples for further discussion below.

Site 3 is situated in a rural/agricultural area in Saint-Anicet of Québec. The largest seasonal average value occurred in the fall during the measurement period of September 2003–August 2014. Fertilizer application in the late fall (mid- to late October) is very common in Canada (Lillyman et al., 2009). Fertilizer is applied at the time when the turf has stopped growing but is still green. Such a practice can ensure early growing in the following spring. With the late-fall fertilizer application, spring fertilization can be postponed until late May to early June. The fertilizer application usually leads to a sharp increase in atmospheric NH_3 mixing ratio (Lillyman et al., 2009; Yao and Zhang, 2013), and this was indeed observed at Site 3. For example, there was usually one 24 h sample in October having a mixing ratio 1–2 orders of magnitude higher than other samples collected before or after. The on-site sampling was performed every third day, and strong NH_3 emissions associated with fertilization application generally occurred within the initial 3–5 days (Lillyman et al., 2009). Thus, extremely high mixing ratios could be observed on one day in October some years but not every year. The episodes further led to large interannual variations with the value of CV reached 0.19.

Site 2 is located in an urban area in Edmonton. Mixing ratios of atmospheric NH_3 were 2.4 ± 0.6 ppb, and the differences between seasonal average values were only 0.1–0.3 ppb during the period of May 2006–April 2014. However, the seasonal average temperature of $16.7 \pm 1.9\,^{\circ}C$ in summer was much higher than that of $-19.8 \pm 4.5\,^{\circ}C$ in winter. The small seasonal variations in NH_3 mixing ratio at this site were caused by two contrasting factors in winter season. On the one hand, extremely low temperature limited soil and vegetation NH_3 emissions to a level close to negligible (Zhang et al., 2010), as was also seen at Site 1 at ambient temperature less than $-9\,^{\circ}C$ (Hu et al., 2014). On the other hand, NH_3 emissions from industrial and/or non-industrial anthropogenic sources seemed to be enhanced in winter (Lillyman et al., 2009; Behera et al., 2013), as was supported by the 2–4 times higher mixing ratios of SO_2, HONO, and HNO_3 in winter than in summer.

3.2 Temporal variations of atmospheric NH_3 at the eight American sites

For the eight AMoN sites in the United States, the data measured from August 2008 to July 2015 were used for analysis at all the sites except at Site 12 for which the data measured during the period of September 2008–August 2015 were used (Fig. 3 and Table 1). Site 7 is located at an intensive agricultural activity zone in Randall, Texas, and Sites 8–10 are located in rural areas in Dodge, Wisconsin; Wayne, Michigan;

Table 1. The mixing ratios of NH_3 at 14 sites (NH_3 unit in ppb, T unit in °C, Sites 1–5, Site 6 and Sites 7–14 belong to NAPS, CAPMoN and AMoN; urban Sites 1–2 and 4–5; rural/agricultural Sites 3, 6, 7–10; remote Sites 11–14).

Site	Sampling period	Annual	Spring		Summer		Fall		Winter		Location		Elevation
		NH_3	NH_3	T	NH_3	T	NH_3	T	NH_3	T	Latitude	Longitude	
1	Jul 2003–Jun 2014	2.6 ± 1.2	2.8 ± 1.2	8.0 ± 6.0	3.7 ± 0.7	21.6 ± 1.5	2.8 ± 0.7	11.8 ± 5.7	1.3 ± 0.6	−2.5 ± 3.1	43.66	−79.40	122
2	May 2006–Apr 2014	2.4 ± 0.6	2.3 ± 0.6	3.7 ± 7.4	2.4 ± 0.4	16.7 ± 1.9	2.6 ± 0.6	4.2 ± 7.7	2.3 ± 0.9	−19.8 ± 4.5	53.49	−113.46	682
3	Sep 2003–Aug 2014	2.1 ± 2.0	1.6 ± 0.8	6.1 ± 6.7	3.0 ± 1.5	19.5 ± 2.2	3.2 ± 2.8	9.1 ± 5.6	0.5 ± 0.3	−6.8 ± 2.9	45.12	−74.29	50
4	Nov 2007–Oct 2014	1.9 ± 0.8	1.7 ± 0.7	8.3 ± 6.9	2.7 ± 0.5	21.5 ± 2.1	2.1 ± 0.4	9.4 ± 6.3	1.0 ± 0.2	−6.1 ± 2.6	45.43	−75.68	72
5	Sep 2003–Aug 2014	1.6 ± 0.5	1.5 ± 0.4	10.1 ± 2.9	1.9 ± 0.4	17.8 ± 1.9	1.7 ± 0.5	10.6 ± 4.1	1.4 ± 0.4	4.2 ± 1.5	49.22	−122.99	122
6	Aug 2003–Jul 2011	0.8 ± 0.6	1.0 ± 0.7	6.7 ± 5.8	1.2 ± 0.4	19.4 ± 2.2	0.7 ± 0.3	9.7 ± 5.3	0.2 ± 0.2	−5.6 ± 2.8	44.23	−79.78	253
7	Aug 2008–Jul 2015	4.9 ± 1.2	4.6 ± 1.2	14.2 ± 4.2	5.5 ± 0.8	25.5 ± 1.7	4.7 ± 1.5	14.7 ± 5.3	4.6 ± 1.4	3.0 ± 1.8	34.88	−101.67	1057
8	Aug 2008–Jul 2015	2.6 ± 1.4	3.2 ± 1.2	7.4 ± 6.5	3.8 ± 0.9	20.7 ± 1.8	2.5 ± 0.6	9.3 ± 5.9	1.0 ± 0.5	−7.4 ± 3.8	43.47	−88.62	287
9	Aug 2008–Jul 2015	2.2 ± 1.0	2.6 ± 1.0	10 ± 6.1	3.2 ± 0.7	22.4 ± 1.7	2.1 ± 0.7	11.5 ± 5.5	1.1 ± 0.3	−3.2 ± 3.3	42.25	−83.20	180
10	Aug 2008–Jul 2015	1.6 ± 1.0	2.3 ± 1.0	11.3 ± 5.7	1.9 ± 0.4	22.1 ± 1.5	1.8 ± 0.8	11.2 ± 5.6	0.4 ± 0.4	−3.3 ± 3.3	40.05	−88.37	212
11	Aug 2008–Jul 2015	0.5 ± 0.4	0.7 ± 0.4	6.6 ± 6.5	0.8 ± 0.3	18.4 ± 1.5	0.3 ± 0.2	9.2 ± 5.0	0.1 ± 0.1	−4.9 ± 3.4	42.40	−72.66	503
12	Sep 2008–Aug 2015	0.3 ± 0.3	0.3 ± 0.2	3.4 ± 6.1	0.5 ± 0.3	17.5 ± 2.6	0.3 ± 0.3	5.5 ± 6.7	0.1 ± 0.1	−13 ± 4.5	47.95	−91.50	524
13	Aug 2008–Jul 2015	0.3 ± 0.4	0.2 ± 0.2	11 ± 3.6	0.7 ± 0.5	23.8 ± 1.5	0.2 ± 0.2	12.5 ± 6.0	0.2 ± 0.1	0.2 ± 2.3	32.94	−72.66	1
14	Aug 2008–Jul 2015	0.3 ± 0.3	0.4 ± 0.2	18.6 ± 4.2	0.5 ± 0.3	27.8 ± 1.0	0.2 ± 0.2	19.7 ± 4.8	0.2 ± 0.2	10.3 ± 3.2	36.81	−107.65	1972

and Champaign, Illinois; respectively, with moderately intensive agricultural activities. Long-term average of NH_3 was as high as 4.9 ± 1.2 ppb at Site 7 where the seasonal average in summer was approximately 20 % higher than those in the other seasons. The M–K analysis result showed an increasing trend at this site with a confidence level of 99.9 %. Long-term averages of NH_3 at Sites 8–10 were 2.6 ± 1.4, 2.2 ± 1.0, and 1.6 ± 1.0 ppb, respectively, and distinctive seasonal variations were seen at the three sites with the lowest values in winter. The M–K analysis results showed an increasing trend at Sites 9–10 with a confidence level of > 98 % and no trend at Site 8.

Sites 11–14 are located in the remote areas in Tompkins, New York; Minnesota Lake, Minnesota; Charleston, South Carolina; and Rio Arriba, New Mexico, respectively. The long-term average NH_3 was only 0.3–0.5 ppb at these four remote sites but with distinctive seasonal variations with the highest in summer and the lowest in winter (Table 1). The M–K analysis results showed an increasing trend at the four sites with a confidence level of > 95 %.

3.3 Exponential correlations between NH_3 and T

When local soil and vegetation emissions were the major contributors to atmospheric NH_3, its mixing ratio usually exhibited an exponential function of ambient T (Sutton et al., 2009; Flechard et al., 2013; Hu et al., 2014). Thus, the exponential correlation relationship was examined at the 14 sites to identify potential major contributors to atmospheric NH_3. Note that a perfect exponential correlation with $R^2 > 0.9$ would occur only when the soil–air mass transfer of NH_3 was not the limitation factor (Flechard et al., 2013; Hu et al., 2014), and soil–air mass transfer rate associated with dry soil was much smaller (Su et al., 2011).

A moderately good exponential correlation was obtained at Site 1 with $R^2 = 0.74$ and P value < 0.01 (Fig. S2a). NH_3 emissions from green space surrounding this site likely played a major role in the observed NH_3 level (Hu et al., 2014). Similar results were obtained at Sites 3, 4, and 6 when a few exterior data points were excluded. For example, five data points at Site 3 severely deviate from the regression curve because of fertilizer application (Fig. S2c). When these five data points were excluded, R^2 reached 0.60 and P value < 0.01. In addition, R^2 was 0.75 at the rural Site 6 when one outlier data point was excluded (Fig. S2f). The two parameters in the regression equation $[NH_3] = 0.24 \times \exp(0.094 \times T)$ were largely different from those obtained at the two downtown sites, i.e., $[NH_3] = 1.48 \times \exp(0.048 \times T)$ at Site 1 and $[NH_3] = 1.29 \times \exp(0.036 \times T)$ at Site 4, noting that the parameters were close between the two downtown sites. Under the condition of T below or close to 0 °C, the mixing ratios of atmospheric NH_3 at the rural Site 6 were almost 1 order of magnitude smaller than those at the downtown sites, leading to the large difference for parameters in regression equations between the rural and urban sites. The

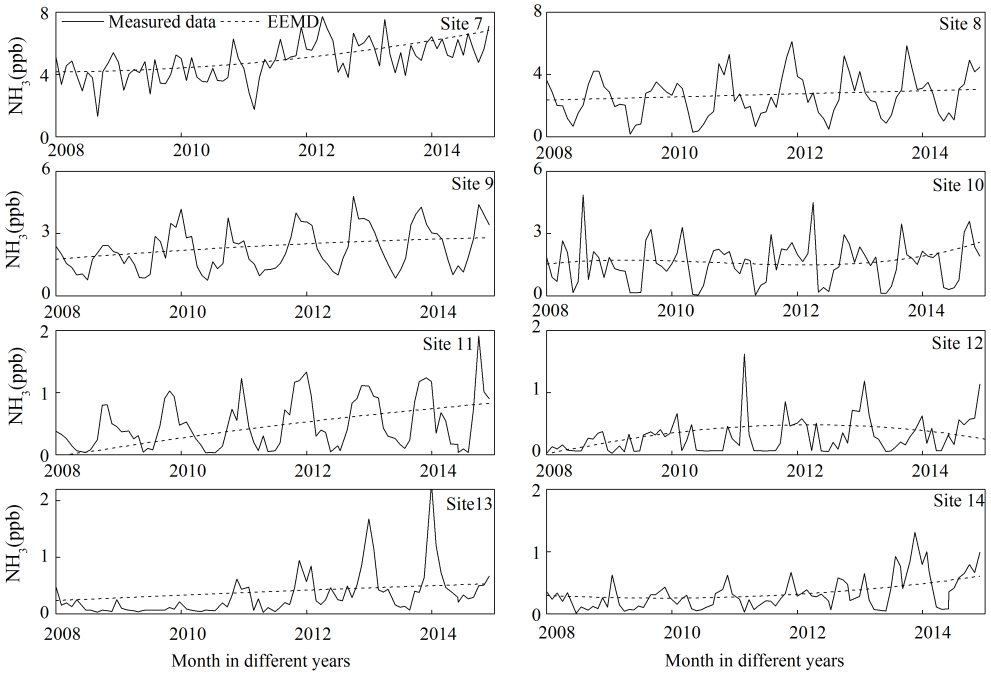

Figure 3. Monthly averages of measured atmospheric NH_3 and its long-term trends extracted by the EEMD at eight US sites.

higher mixing ratio under freezing conditions at the Toronto downtown site was proposed to be likely associated with NH_3 emissions from green space (Hu et al., 2014). Flechard et al. (2013) also reported higher NH_3 mixing ratios over a grassland under freezing conditions, which could be due to slower dry deposition process and/or shallow boundary layer.

At Site 2, the exponential correlation was poor even with two outlier samples being excluded (Fig. S2b), implying that local soil and vegetation emissions were less likely the major contributors to atmospheric NH_3. Like Site 2, R^2 was only 0.39 at Site 5 even with two exterior data points being excluded (Fig. S2e). NH_3 in urban atmospheres was reported to come from various sources (Whitehead et al., 2007; Ianniello et al., 2010; Saylor et al., 2010; Meng et al., 2011; Reche et al., 2012), some of which were less dependent on ambient T.

R^2 between atmospheric NH_3 and ambient T was below 0.1 at Site 7 (Fig. S3a). Considering the high mixing ratios observed at the rural/agricultural site, it can be confirmed that local agricultural emissions were the major contributor to atmospheric NH_3 and the agricultural emissions appeared to be independent on ambient T. R^2 of 0.64, 0.69, and 0.45 at Sites 8–10, respectively (Fig. S3b–d), suggested that local soil and vegetation emissions should be among the major contributors to atmospheric NH_3. The same can be said for the remote Site 11 with R^2 of 0.63 (Fig. S3e). R^2 was 0.25, 0.2, and 0.15 at remote Sites 12–14 (Fig. S3f–i), respectively. When the data measured in calendar year 2011, 2012, 2013, and 2014 at Site 13 were used for correlation analysis, respectively, the values of R^2 were 0.47 in 2011, 0.58 in 2012, 0.69 in 2013, and 0.74 in 2014. Local soil and vegetation emissions might be among the major contributors to atmospheric NH_3 at the site while the low R^2 values in 2011–2012 could be due to analytical errors. In fact, the mixing ratios at the site in 2011–2012 were generally close to the detection limit. A similar calculation was conducted at Site 14 with R^2 still below 0.2 in different calendar years, suggesting that local soil and vegetation emissions were unlikely the major contributors to atmospheric NH_3. Yao and Zhang (2013) proposed that long-range transport could be an important contributor to atmospheric NH_3 at remote sites in North America. When a similar calculation was conducted at Site 12, R^2 was 0.57 in 2012, 0.81 in 2013, and 0.39 in 2014. Local soil and vegetation emissions were possibly among the major contributors to atmospheric NH_3 at the site in 2012 and 2013, but the long-range transport together with local soil and vegetation emissions might be important contributors to atmospheric NH_3 in 2014.

3.4 Cause analysis of trends in atmospheric NH_3 at Canadian sites

Site 1 is located in Downtown Toronto, Ontario. Figure S4a shows the annual anthropogenic NH_3 emissions from 2003 to 2013 in Ontario, Canada. Not only the total NH_3 emissions, but also emissions from the four major sectors including agricultural, mobile, industrial, and non-industrial generally decreased. However, an increasing trend in annual average NH_3 was found at Site 1, which was identified to be caused by (1) the increased T and (2) the decreased SO_2 emission. Increasing T not only increases soil and vegeta-

tion NH_3 emissions but also favors more NH_3 partitioning in the gas phase (Pinder et a., 2012; Sutton et al., 2013); both processes would increase NH_3 mixing ratios. The decreased SO_2 emissions due to the tightened emission control policies since 2008 by the city and provincial governments led to significant declines in SO_2 oxidation products (Hu et al., 2014; Pugliese et al., 2014), which in turn also affected NH_3–pNH_4^+ partitioning, the surface resistance for NH_3, and increased NH_3 mixing ratios (Yao et al., 2007; Fowler et al., 2015). These hypotheses were supported by the trends in T and pNH_4^+ and their correlations with that in NH_3, as detailed below.

A moderately good correlation ($R^2 = 0.76$, P value < 0.01) was obtained between the annual average NH_3 and the annual average T, while a negative correlation ($R^2 = 0.40$ and P value < 0.05) was obtained between the annual average NH_3 and pNH_4^+ (Fig. 4a). Note that a decreasing trend in annual average pNH_4^+ was found with a confidence level of $> 99\,\%$ based on M–K analysis. When ambient T was increased by 5 °C, the mixing ratio of atmospheric NH_3 was increased by ~ 1 ppb according to the regression equation. The annual average T shown in Fig. 4 was calculated from the daily averaged values of T on the sampling days when valid NH_3 data were available, not every day of the year, and thus might be different from the actual annual average T. The moderately good correlation between the annual average values of NH_3 and ambient temperature might be coincident. This is also supported by the decreasing correlation when the EEMD-extracted results were used for calculation as presented below.

Figure S5 shows the intrinsic mode functions (IMFs) and residuals solved by the EEMD at Site 1. The extracted residuals represented the long-term trend in atmospheric NH_3, and the IMFs represented other fluctuations in different timescales. The EEMD-extracted long-term trend in atmospheric NH_3 was generally increased by $\sim 20\,\%$ from 2003 to 2014. The EEMD was also used to extract the long-term trend in pNH_4^+ in $PM_{2.5}$ from 2003 to 2014 (Fig. S6). Correlation between the two EEMD-extracted long-term trends resulted in a regression equation of $[NH_3] = -1.41 \times [pNH_4^+] + 4.3$, with $R^2 = 0.93$ and P value < 0.01 (Fig. 4b). The unit of NH_3 is in ppb while the unit of pNH_4^+ is in $\mu g\,m^{-3}$. The absolute value of the regression slope was almost the same as the unit conversion coefficient. Thus, the EEMD-extracted long-term trend in atmospheric NH_3 seemed to be mainly determined by the change in NH_3–pNH_4^+ partitioning. The increasing T further enhanced this trend. When the EEMD-extracted long-term trend in ambient T was correlated to that of atmospheric NH_3, we obtained $[NH_3] = 0.13 \times T + 1.5$, $R^2 = 0.47$ and P value < 0.01 (Fig. 4b). The EEMD-extracted results suggest that the change in NH_3–NH_4^+ partitioning is one of the dominant factors influencing the long-term NH_3 trend at Site 1. The relative importance between (1) changes in NH_3–NH_4^+ partitioning and (2) increased bio-

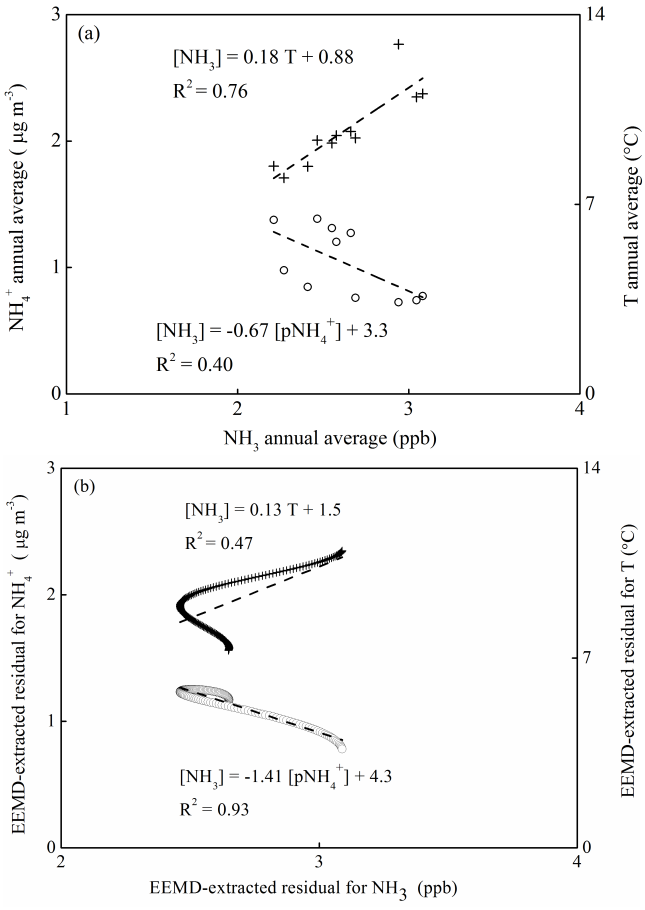

Figure 4. Correlations between atmospheric NH_3 and ambient T at Site 1 (**a**: annual average value; **b**: EEMD-extracted trend).

genic NH_3 emission due to increasing T is yet to be investigated.

At Site 2, the EEMD-extracted residual of atmospheric NH_3 varied within a very small range ($\sim 10\,\%$, Fig. 2), which was consistent with stable trend generated from the M–K analysis. Little correlation was found between the annual average NH_3 and T ($R^2 < 0.05$) or pNH_4^+ ($R^2 < 0.01$). Thus, the NH_3 trend identified at Site 2 was seemingly unaffected by changes in NH_3–NH_4^+ partitioning and T-dependent biogenic NH_3 emission, or additional local factors canceled out the impact from the two factors.

Site 3 is a rural/agricultural site and annual agricultural NH_3 emissions in Québec were stable from 2003 to 2009 with a CV of 0.02 (Fig. S4c). During the same period, mobile, industrial, and non-industrial emissions were decreased by 40 % in Québec. While the M–K analysis result showed no consistent long-term trend in atmospheric NH_3, the EEMD-extracted a bell-shaped pattern (Fig. 2). That is, NH_3 increased from 1.7 ppb in 2003 to 2.5 ppb in 2009 and then decreased down to 1.3 ppb in 2014. The anthropogenic NH_3 emission data from 2003 to 2009 did not support the

increasing trend in atmospheric NH_3 at this site during this period. However, Sintermann et al. (2012) reported that NH_3 emission factors highly depend on meteorology and efficiencies of technical controls on NH_3 emission processes. NH_3 emission factors adopted in NH_3 emission inventories may suffer from uncertainties to some extent, which in turn may transfer to the estimated NH_3 emission and affect its relationship with the observed atmospheric NH_3.

A good correlation was found between the EEMD-extracted long-term trends in NH_3 and T with a linear regression relationship of $[NH_3] = 0.39 \times T - 0.30$, with $R^2 = 0.80$ and P value < 0.01. The slope of 0.39 was consistent with that reported by Sutton et al. (2013). That is, NH_3 volatilization potential nearly doubles every 5 °C. On the contrary, little correlation was found between the EEMD-extracted residuals for atmospheric NH_3 and pNH_4^+ ($R^2 < 0.1$), suggesting that the NH_3–pNH_4^+ partitioning likely played a negligible role on the long-term trend in atmospheric NH_3 at this site.

A similar conclusion could also be generated for Site 4 to that for Site 3. The M–K analysis results showed a stable trend in atmospheric NH_3 and a slightly decreasing trend in pNH_4^+ with a confidence level of > 99 %. The EEMD-extracted long-term trend showed that NH_3 decreased by ∼ 5 % from 2007 to 2008 and then increased by ∼ 50 % afterwards. Although the correlation between the annual averages NH_3 and T was not very good ($R^2 = 0.39$, $P = 0.13$), correlation between the EEMD-extracted long-term trends in NH_3 and T was almost perfect ($R^2 = 0.90$, $P < 0.01$). No correlation was found between the annual average NH_3 and $[pNH_4^+]$ ($R^2 < 0.01$), and a relatively low correlation was found between the EEMD-extracted long-term trends in atmospheric NH_3 and pNH_4^+ ($R^2 = 0.39$, P value < 0.01). These results suggested that the long-term change in ambient T possibly affected the long-term trend in atmospheric NH_3 at the site. However, longer measurements are still needed to confirm the trends in atmospheric NH_3 and ambient T as well as their relationship at the site because of the inherent weaknesses in this data set, such as only 7 years and only one 24 h sample every 3 days available data, and some missing data during this period.

Site 5 is an urban site located in British Columbia, Canada. Anthropogenic NH_3 emissions were decreased from 2003 to 2013 in this province (Fig. S4c). The M–K analysis result showed no trend in atmospheric NH_3 at Site 5 from 2003 to 2014, and the EEMD-extracted long-term trend was almost constant. We conducted the correlation analysis of the EEMD-extracted results and found that the long-term changes in ambient T and pNH_4^+ cannot explain the EEMD-extracted trend in atmospheric NH_3 at this site.

At Site 6, the EEMD-extracted trend in atmospheric NH_3 showed an increase of ∼ 10 % from 2003 to 2006 and then a decrease of ∼ 40 % afterwards (Fig. 2). Poor correlations were found between annual average NH_3 and T or between NH_3 and NH_4^+ with P values > 0.05. Meaningless correlations between the EEMD-extracted trends in NH_3 and T or between the EEMD-extracted trends in NH_3 and NH_4^+ were obtained. The trend in T and NH_3–NH_4^+ partitioning cannot explain the long-term variations of atmospheric NH_3.

3.5 Cause analysis of trends in atmospheric NH_3 at the US sites

At the eight US sites, R^2 values between annual average NH_3 and T were all below 0.2 with P values all larger than 0.1. The simple correlation analysis did not provide direct evidence that T was the significant factor affecting the NH_3 trend. However, the EEMD-extracted trends in NH_3 and T had a much better correlation at some sites, e.g., with $R^2 = 0.85$, 0.99, 0.54, and 0.99 at Sites 7, 8, 9, and 13, respectively, and with P values smaller than 0.01. Thus, the increasing T was likely one of important factors causing the long-term trend in NH_3 at these four sites. Note that no reasonable relationship was identified between trends in NH_3 and T at the other four sites using the EEMD method.

The EEMD-extracted long-term trend showed an increase in atmospheric NH_3 from 4.2 ppb in August 2008 to 6.8 ppb in July 2015 at Site 7 (Fig. 3a), from 2.4 ppb in August of 2008 to 3.0 ppb in July of 2015 at Site 8 (Fig. 3b), from 1.8 ppb in August of 2008 to 2.8 ppb in July of 2015 at Site 9 (Fig. 3c), a complex varying pattern during the period from August 2008 to July 2015 at Site 10 (Fig. 3d), and an increasing trend (by 0.3–0.5 ppb, or 100–200 % in percentages) at Sites 11–14 (Fig. 3e–h). The percentage increases (100–200 %) in NH_3 mixing ratio from 2008 to 2015 at the remote sites were substantially larger than those at the rural/agricultural sites (20–50 %).

NH_3 emissions in the United States increased by 11 % during the period from 1990 to 2010 due to the growth of livestock activities (Xing et al., 2013). This is particularly the case in North Carolina and Iowa. This increase alone is not enough to explain the ∼ 50 % increase in NH_3 from 2008 to 2015 at Site 7, which is located in Texas. The increased T is possibly another important factor causing the increased NH_3 at this site, as mentioned above. It is also noted that the increasing trends in NH_3 at Sites 11–14 identified using the EEMD-extracted results were also consistent with the M–K analysis results.

The annual average NH_3 at the remote sites reached 0.4–0.6 ppb in 2015. Assuming the same increasing rate continues for another 7–10 years, the annual average will exceed the proposed critical level of 1 $\mu g\, m^{-3}$ at two sites for protecting sensitive ecosystems (Cape et al., 2009).

4 Conclusions

Long-term average of atmospheric NH_3 was in the range of 0.3–0.5, 1.6–2.6, and 0.8–4.9 ppb at the remote, ur-

ban, and rural/agricultural sites across North America, respectively. Moderate exponential correlations between atmospheric NH_3 and ambient T were found at nine sites, implying that local biogenic emissions and/or NH_3–NH_4^+ partitioning were likely important factors causing the long-term trends in atmospheric NH_3 at these sites. However, the length of the used data covers only 7–11 years, and further examination is needed for the trend analysis when more data of atmospheric NH_3 are available.

No decreasing trends in atmospheric NH_3 were found at the four Canadian sites despite significant decreases in anthropogenic NH_3 emissions from main sectors in the last decade. The decreased NH_3 anthropogenic emission was compensated for or overwhelmed by the increased biogenic emission, changes in NH_3–NH_4^+ partitioning, and/or the increased surface resistance for NH_3 because of the less acidic surface associated with less SO_2 dry deposition. This was supported by pNH_4^+ data which exhibited a decreasing trend, likely caused by a combination of reduced SO_2 and NO_x emission and increased temperature. No decreasing trends in atmospheric NH_3 were found at other two Canadian sites, but it was unknown what caused this phenomenon. Uncertainties in the NH_3 emission inventory are still a concern and may affect the trend analysis results of the relationship between atmospheric NH_3 and NH_3 emissions.

The M–K analysis showed an increasing trend in atmospheric NH_3 at seven out of the eight US sites, which was also supported by the EEMD-extracted results. NH_3 increased by 20–50 % from 2008 to 2015 at the three rural/agricultural sites and by 100–200 % at the four remote sites. If the same increasing trend continues in the next 5–7 years, the annual average NH_3 at two remote sites will exceed $1\,\mu g\,m^{-3}$, a level below which has been proposed to protect sensitive ecosystems at the remote sites.

In most cases, the two statistical approaches used in the present study yield consistent trends in atmospheric NH_3 measured at different sites. The EEMD method appeared to have more powerful interpretation ability for resolving trends because (1) it is less affected by extremely high concentration points, and (2) it yields a continuous and quantitative trend result. However, this method occasionally suffers from "the end effect" and leads to physically meaningless results. Using the combined approach (or more than one statistical methods) can better resolve and interpret long-term trends in atmospheric NH_3.

5 Data availability

The emission date of NH_3 can be downloaded at the link http://www.ec.gc.ca/inrp-npri/default.asp?lang=En&n=4A577BB9-1 (NPRI, 2016). The data of atmospheric NH_3 measured by the Canadian National Air Pollution Surveillance (NAPS) can be downloaded from http://www.ec.gc.ca/rnspa-naps/ (NAPS, 2016). The data of atmospheric NH_3 measured by the Canadian Air and Precipitation Monitoring Network (CAPMoN) can be downloaded from http://www.ec.gc.ca/natchem/default.asp?lang=En&n=90EDB4BC-1 (CAPMoN, 2016) by sending a request email to national.atmospheric.chemistry.ontario@ec.gc.ca; The data of atmospheric NH_3 measured by the US Passive Ammonia Monitoring Network can be downloaded from http://nadp.sws.uiuc.edu/AMoN (Gay et al., 2016).

The Supplement related to this article is available online at doi:10.5194/acp-16-11465-2016-supplement.

Acknowledgements. Ammonia Monitoring Network (http://nadp.sws.uiuc.edu/data/sites/list/?net=AMoN) is acknowledged for allowing the use of the data for analysis conducted in this study. The work is financially supported by the Clear Air Regulatory Agenda of Canada and Xiaohong Yao thanks the support from the National Program on Key Basic Research Project (973 Program: 2014CB953700) of China.

Edited by: F. Yu
Reviewed by: C. R. Flechard and one anonymous referee

References

Alebic-Juretic, A.: Airborne ammonia and ammonium within the Northern Adriatic area, Croatia, Environ. Pollut., 154, 439–447, doi:10.1016/j.envpol.2007.11.029, 2008.

Beem, K. B., Raja, S., Schwandner, F. M., Taylor, C., Lee, T., Sullivan, A. P., Carrico, C. M., McMeeking, G. R., Day, D., and Levin, E.: Deposition of reactive nitrogen during the Rocky Mountain Airborne Nitrogen and Sulfur (RoMANS) study, Environ. Pollut., 158, 862–872, doi:10.1016/j.envpol.2009.09.023, 2010.

Behera, S. N., Sharma, M., Aneja, V. P., and Balasubramanian, R.: Ammonia in the atmosphere: a review on emission sources, atmospheric chemistry and deposition on terrestrial bodies, Environ. Sci. Pollut. R., 20, 8092–8131, doi:10.1007/s11356-013-2051-9, 2013.

Bishop, G. A., Peddle, A. M., Stedman, D. H., and Zhan, T.: On-road emission measurements of reactive nitrogen compounds from three California cities, Environ. Sci. Technol., 44, 3616–3620, doi:10.1021/es903722p, 2010.

Bobbink, R., Hicks, K., Galloway, J., Spranger, T., Alkemade, R., Ashmore, M., Bustamante, M., Cinderby, S., Davidson, E., and Dentener, F.: Global assessment of nitrogen deposition effects on terrestrial plant diversity: a synthesis, Ecol. Appl., 20, 30–59, doi:10.1890/08-1140.1, 2010.

Canadian Air and Precipitation Monitoring Network (CAPMoN): The NAtChem Data, data updated annually, available at: http://www.ec.gc.ca/natchem/default.asp?lang=En&n=90EDB4BC-1, last access: 12 September 2016.

Cape, J. N., Van der Eerden, L. J., Sheppard, L. J., Leith, I. D., and Sutton, M. A.: Evidence for changing the critical level for ammonia, Environ. Pollut., 157, 1033–1037, doi:10.1016/j.envpol.2008.09.049, 2009.

Dabek-Zlotorzynska, E., Dann, T. F., Martinelango, P. K., Celo, V., Brook, J. R., Mathieu, D., Ding, L., and Austin, C. C.: Canadian National Air Pollution Surveillance (NAPS) $PM_{2.5}$ speciation program: methodology and $PM_{2.5}$ chemical composition for the years 2003–2008, Atmos. Environ., 45, 673–686, doi:10.1016/j.atmosenv.2010.10.024, 2011.

Day, D. E., Chen, X., Gebhart, K. A., Carrico, C. M., Schwandner, F. M., Benedict, K. B., Schichtel, B. A., and Collett, J. L.: Spatial and temporal variability of ammonia and other inorganic aerosol species, Atmos. Environ., 61, 490–498, doi:10.1016/j.atmosenv.2012.06.045, 2012.

Ellis, R. A., Murphy, J. G., Markovic, M. Z., VandenBoer, T. C., Makar, P. A., Brook, J., and Mihele, C.: The influence of gas-particle partitioning and surface-atmosphere exchange on ammonia during BAQS-Met, Atmos. Chem. Phys., 11, 133–145, doi:10.5194/acp-11-133-2011, 2011.

Erisman, J. W., Bleeker, A., Galloway, J., and Sutton, M. S.: Reduced nitrogen in ecology and the environment, Environ. Pollut., 150, 140–149, doi:10.1016/j.envpol.2007.06.033, 2007.

Erturk, A., Gullu, M. K., and Erturk, S.: Hyperspectral image classification using empirical mode decomposition with spectral gradient enhancement, IEEE T. Geosci. Remote, 51, 2787–2798, doi:10.1109/TGRS.2012.2217501, 2013.

Ferm, M. and Hellsten, S.: Trends in atmospheric ammonia and particulate ammonium concentrations in Sweden and its causes, Atmos. Environ., 61, 30–39, doi:10.1016/j.atmosenv.2012.07.010, 2012.

Flechard, C. R., Massad, R.-S., Loubet, B., Personne, E., Simpson, D., Bash, J. O., Cooter, E. J., Nemitz, E., and Sutton, M. A.: Advances in understanding, models and parameterizations of biosphere-atmosphere ammonia exchange, Biogeosciences, 10, 5183–5225, doi:10.5194/bg-10-5183-2013, 2013.

Fowler, D., Steadman, C. E., Stevenson, D., Coyle, M., Rees, R. M., Skiba, U. M., Sutton, M. A., Cape, J. N., Dore, A. J., Vieno, M., Simpson, D., Zaehle, S., Stocker, B. D., Rinaldi, M., Facchini, M. C., Flechard, C. R., Nemitz, E., Twigg, M., Erisman, J. W., Butterbach-Bahl, K., and Galloway, J. N.: Effects of global change during the 21st century on the nitrogen cycle, Atmos. Chem. Phys., 15, 13849–13893, doi:10.5194/acp-15-13849-2015, 2015.

Gay, D., Claybrooke, R., Larson, B., Rhodes, M., Volk, L., and Lehmann, C.: Ammonia Monitoring Network (AMoN), National Atmospheric Deposition Program, data updated monthly or bi-monthly, US Passive Ammonia Monitoring Network, available at: http://nadp.sws.uiuc.edu/AMoN, last access: 12 September 2016.

Gilbert, R. O.: Statistical Methods for Environmental Pollution Monitoring, John Wiley & Sons, New York, USA, 1987.

Hand, J. L., Schichtel, B. A., Pitchford, M., Malm, W. C., and Frank, N. H.: Seasonal composition of remote and urban fine particulate matter in the United States, J. Geophys. Res.-Atmos., 117, D05209, doi:10.1029/2011JD017122, 2012.

Hu, Q., Zhang, L., Evans, G. J., and Yao, X.: Variability of atmospheric ammonia related to potential emission sources in downtown Toronto, Canada, Atmos. Environ., 99, 365–373, doi:10.1016/j.atmosenv.2014.10.006, 2014.

Ianniello, A., Spataro, F., Esposito, G., Allegrini, I., Rantica, E., Ancora, M. P., Hu, M., and Zhu, T.: Occurrence of gas phase ammonia in the area of Beijing (China), Atmos. Chem. Phys., 10, 9487–9503, doi:10.5194/acp-10-9487-2010, 2010.

Ianniello, A., Spataro, F., Esposito, G., Allegrini, I., Hu, M., and Zhu, T.: Chemical characteristics of inorganic ammonium salts in $PM_{2.5}$ in the atmosphere of Beijing (China), Atmos. Chem. Phys., 11, 10803–10822, doi:10.5194/acp-11-10803-2011, 2011.

Kampata, J. M., Parida, B. P., and Moalafhi, D. B.: Trend analysis of rainfall in the headstreams of the Zambezi River Basin in Zambia, Phys. Chem. Earth., 33, 621–625, doi:10.1016/j.pce.2008.06.012, 2008.

Krupa, S. V.: Effects of atmospheric ammonia (NH_3) on terrestrial vegetation: a review, Environ. Pollut., 124, 179–221, doi:10.1016/S0269-7491(02)00434-7, 2003.

Kulmala, M., Vehkamäki, H., Petäjä, T., Dal Maso, M., Lauri, A., Kerminen, V., Birmili, W., and McMurry, P. H.: Formation and growth rates of ultrafine atmospheric particles: a review of observations, J. Aerosol. Sci., 35, 143–176, doi:10.1016/j.jaerosci.2003.10.003, 2004.

Lillyman, C., Buset, K., and Mullins, D.: Canadian Atmospheric Assessment of Agricultural Ammonia, National Agri-Environmental Standards, Environment Canada, Gatineau, Quebec, Canada, 2009.

Markovic, M. Z., VandenBoer, T. C., Baker, K. R., Kelly, J. T., and Murphy, J. G.: Measurements and modeling of the inorganic chemical composition of fine particulate matter and associated precursor gases in California's San Joaquin Valley during CalNex 2010, J. Geophys. Res.-Atmos., 119, 6853–6866, doi:10.1002/2013JD021408, 2014.

Meng, Z. Y., Lin, W. L., Jiang, X. M., Yan, P., Wang, Y., Zhang, Y. M., Jia, X. F., and Yu, X. L.: Characteristics of atmospheric ammonia over Beijing, China, Atmos. Chem. Phys., 11, 6139–6151, doi:10.5194/acp-11-6139-2011, 2011

National Air Pollution Surveillance Program (NAPS): Atmospheric NH_3, data updated monthly or bi-monthly, available at: http://www.ec.gc.ca/rnspa-naps/, last access: 12 September 2016.

Nowak, J. B., Neuman, J. A., Bahreini, R., Middlebrook, A. M., Holloway, J. S., McKeen, S. A., Parrish, D. D., Ryerson, T. B., and Trainer, M.: Ammonia sources in the California South Coast Air Basin and their impact on ammonium nitrate formation, Geophys. Res. Lett., 39, L07804, doi:10.1029/2012GL051197, 2012.

National Pollutant Release Inventory (NPRI): Emission date of NH_3, data update annually, available at: http://www.ec.gc.ca/inrp-npri/default.asp?lang=En&n=4A577BB9-1, last access: 12 September 2016.

Paulot, F. and Jacob, D. J.: Hidden cost of US agricultural exports: particulate matter from ammonia emissions, Environ. Sci. Technol., 48, 903–908, doi:10.1021/es4034793, 2014.

Pinder, R. W., Davidson, E. A., Goodale, C. L., Greaver, T. L., Herrick, J. D., and Liu, L.: Climate change impacts of US reactive nitrogen, P. Natl. Acad. Sci. USA, 109, 7671–7675, doi:10.1073/pnas.1114243109, 2012.

Puchalski, M. A., Rogers, C. M., Baumgardner, R., Mishoe, K. P., Price, G., Smith, M. J., Watkins, N., and Lehmann, C. M.: A statistical comparison of active and passive ammonia measurements collected at Clean Air Status and Trends Net-

work (CASTNET) sites, Environ. Sci.-Proc. Imp., 17, 358–369, doi:10.1039/c4em00531g, 2015.

Pugliese, S. C., Murphy, J. G., Geddes, J. A., and Wang, J. M.: The impacts of precursor reduction and meteorology on ground-level ozone in the Greater Toronto Area, Atmos. Chem. Phys., 14, 8197–8207, doi:10.5194/acp-14-8197-2014, 2014.

Pye, H., Liao, H., Wu, S., Mickley, L. J., Jacob, D. J., Henze, D. K., and Seinfeld, J. H.: Effect of changes in climate and emissions on future sulfate-nitrate-ammonium aerosol levels in the United States, J. Geophys. Res.-Atmos., 114, D01205, doi:10.1029/2008JD010701, 2009.

Reche, C., Viana, M., Pandolfi, M., Alastuey, A., Moreno, T., Amato, F., Ripoll, A., and Querol, X.: Urban NH_3 levels and sources in a Mediterranean environment, Atmos. Environ., 57, 153–164, doi:10.1016/j.atmosenv.2012.04.021, 2012.

Ren, H., Wang, Y., Huang, M., Chang, Y., and Kao, H.: Ensemble empirical mode decomposition parameters optimization for spectral distance measurement in hyperspectral remote sensing data, Remote Sens., 6, 2069–2083, doi:10.3390/rs6032069, 2014.

Saylor, R. D., Edgerton, E. S., Hartsell, B. E., Baumann, K., and Hansen, D. A.: Continuous gaseous and total ammonia measurements from the southeastern aerosol research and characterization (SEARCH) study, Atmos. Environ., 44, 4994–5004, doi:10.1016/j.atmosenv.2010.07.055, 2010.

Schiferl, L. D., Heald, C. L., Nowak, J. B., Holloway, J. S., Neuman, J. A., Bahreini, R., Pollack, I. B., Ryerson, T. B., Wiedinmyer, C., and Murphy, J. G.: An investigation of ammonia and inorganic particulate matter in California during the CalNex campaign, J. Geophys. Res.-Atmos., 119, 1883–1902, doi:10.1002/2013JD020765, 2014.

Sintermann, J., Neftel, A., Ammann, C., Häni, C., Hensen, A., Loubet, B., and Flechard, C. R.: Are ammonia emissions from field-applied slurry substantially over-estimated in European emission inventories?, Biogeosciences, 9, 1611–1632, doi:10.5194/bg-9-1611-2012, 2012.

Su, H., Cheng, Y., Oswald, R., Behrendt, T., Trebs, I., Meixner, F. X., Andreae, M. O., Cheng, P., Zhang, Y., and Pöschl, U.: Soil nitrite as a source of atmospheric HONO and OH radicals, Science, 333, 1616–1618, doi:10.1126/science.1207687, 2011.

Sutton, M. A., Nemitz, E., Theobald, M. R., Milford, C., Dorsey, J. R., Gallagher, M. W., Hensen, A., Jongejan, P. A. C., Erisman, J. W., Mattsson, M., Schjoerring, J. K., Cellier, P., Loubet, B., Roche, R., Neftel, A., Hermann, B., Jones, S. K., Lehman, B. E., Horvath, L., Weidinger, T., Rajkai, K., Burkhardt, J., Löpmeier, F. J., and Daemmgen, U.: Dynamics of ammonia exchange with cut grassland: strategy and implementation of the GRAMINAE Integrated Experiment, Biogeosciences, 6, 309–331, doi:10.5194/bg-6-309-2009, 2009.

Sutton, M. A., Reis, S., Riddick, S. N., Dragosits, U., Nemitz, E., Theobald, M. R., Tang, Y. S., Braban, C. F., Vieno, M., and Dore, A. J.: Towards a climate-dependent paradigm of ammonia emission and deposition, Philos. T. Roy. Soc. B, 368, 20130166, doi:10.1098/rstb.2013.0166, 2013.

Theobald, M. R., Løfstrøm, P., Walker, J., Andersen, H. V., Pedersen, P., Vallejo, A., and Sutton, M. A.: An intercomparison of models used to simulate the short-range atmospheric dispersion of agricultural ammonia emissions, Environ. Modell. Softw., 37, 90–102, doi:10.1016/j.envsoft.2012.03.005, 2012.

Van Damme, M., Clarisse, L., Heald, C. L., Hurtmans, D., Ngadi, Y., Clerbaux, C., Dolman, A. J., Erisman, J. W., and Coheur, P. F.: Global distributions, time series and error characterization of atmospheric ammonia (NH_3) from IASI satellite observations, Atmos. Chem. Phys., 14, 2905–2922, doi:10.5194/acp-14-2905-2014, 2014.

Walker, J. M., Philip, S., Martin, R. V., and Seinfeld, J. H.: Simulation of nitrate, sulfate, and ammonium aerosols over the United States, Atmos. Chem. Phys., 12, 11213–11227, doi:10.5194/acp-12-11213-2012, 2012.

Walker, J. T., Aneja V. P., and Dickey D. A.: Atmospheric transport and wet deposition of ammonium in North Carolina, Atmos. Environ., 34, 3407–3418, doi:10.1016/S1352-2310(99)00499-9, 2000.

Whitehead, J. D., Longley, I. D., and Gallagher, M. W.: Seasonal and diurnal variation in atmospheric ammonia in an urban environment measured using a quantum cascade laser absorption spectrometer, Water Air Soil Pollut., 183, 317–329, doi:10.1007/s11270-007-9381-5, 2007.

Wu, Z. and Huang, N. E.: Ensemble empirical mode decomposition: a noise-assisted data analysis method, Adv. Adapt. Data Anal., 1, 1–41, 2009.

Xing, J., Pleim, J., Mathur, R., Pouliot, G., Hogrefe, C., Gan, C.-M., and Wei, C.: Historical gaseous and primary aerosol emissions in the United States from 1990 to 2010, Atmos. Chem. Phys., 13, 7531–7549, doi:10.5194/acp-13-7531-2013, 2013.

Yao, X., Ling, T. Y., Fang, M., and Chan, C. K.: Size dependence of in situ pH in submicron atmospheric particles in Hong Kong. Atmos. Environ., 41, 382–393, doi:10.1016/j.atmosenv.2006.07.037, 2007.

Yao, X., Hu, Q., Zhang, L., Evans, G. J., Godri, K. J., and Ng, A. C.: Is vehicular emission a significant contributor to ammonia in the urban atmosphere?, Atmos. Environ., 80, 499–506, doi:10.1016/j.atmosenv.2013.08.028, 2013.

Yao, X. H. and Zhang, L.: Supermicron modes of ammonium ions related to fog in rural atmosphere, Atmos. Chem. Phys., 12, 11165–11178, doi:10.5194/acp-12-11165-2012, 2012.

Yao, X. H. and Zhang, L.: Analysis of passive-sampler monitored atmospheric ammonia at 74 sites across southern Ontario, Canada, Biogeosciences, 10, 7913–7925, doi:10.5194/bg-10-7913-2013, 2013.

Zbieranowski, A. L. and Aherne, J.: Long-term trends in atmospheric reactive nitrogen across Canada: 1988–2007, Atmos. Environ., 45, 5853–5862, doi:10.1016/j.atmosenv.2011.06.080, 2011.

Zhang, L., Wright, L. P., and Asman, W.: Bi-directional air-surface exchange of atmospheric ammonia: A review of measurements and a development of a big-leaf model for applications in regional-scale air-quality models, J. Geophys. Res.-Atmos., 115, D20310, doi:10.1029/2009JD013589, 2010.

Zhu, L., Henze, D. K., Cady Pereira, K. E., Shephard, M. W., Luo, M., Pinder, R. W., Bash, J. O., and Jeong, G. R.: Constraining US ammonia emissions using TES remote sensing observations and the GEOS-Chem adjoint model, J. Geophys. Res.-Atmos., 118, 3355–3368, doi:10.1002/jgrd.50166, 2013.